JOURNAL OF MATERIALS SCIENCE: MATERIALS IN MEDICINE 6 (1995) 360–366

Long-term behaviour of a hydroxyapatite/collagen–glycosaminoglycan biomaterial used for oral surgery: a case report

J. HEMMERLE, M. LEIZE, J.-C. VOEGEL
Centre de Recherches Odontologiques, INSERM U.424 Faculté de Chirurgie Dentaire, 1, Place de l'Hôpital-67000 Strasbourg, France

A composite biomaterial consisting of hydroxyapatite with a collagen–glycosaminoglycan coating was studied for evaluation of the osteogenesis after long-term implantation in a human freshly extracted alveolar socket. The ultrastructural investigations were realized using scanning and transmission electron microscopy on cryofractured and embedded biopsy specimens. Crystallographic data were obtained by X-ray diffraction and high resolution transmission electron microscopy. The biomaterial (Biostite®) was shown to consist of irregularly shaped mineral particles of high dispersity, each made up of numerous single hydroxyapatite crystals. In addition, this crystalline phase appeared to be incorporated in a fibrous network. 42 months after implantation only some intercrystalline spaces of the hydroxyapatite aggregates were invested by newly formed bone-like apatite crystals. Moreover, this investigation showed clearly well-mineralized bone interfacing with some implanted aggregates, whereas other hydroxyapatite particles were still surrounded by soft tissue. No evidence of resorption of implanted material was found and the synthetic hydroxyapatite crystals appeared to remain unaltered by long-term implantation.

1. Introduction

Many biomaterials have been proposed with the purpose of promoting osteogenesis. During the last decade the trend has been to develop synthetic biomaterials able to replace bone grafts. Among these synthetic biomaterials, calcium phosphate ceramics have undoubtedly been the most studied and employed in oral and orthopeadic surgery. Numerous authors claim the osteoconductive properties of such ceramics [1–4]. Various applications have been proposed for their use in surgery. In particular, they have already been used for lumen augmentation in laryngotracheal reconstruction [5], or in vertebral arthrodesis [4], and in the dental field mainly in the case of periodontal lesions [1, 2, 6], for pulp capping [7], for the filling of extraction sockets, or for coatings on metals and other substrates.

Synthetic hydroxyapatite is a calcium phosphate ceramic, having a chemical formula $Ca_{10}(PO_4)_6(OH)_2$ and a Ca/P molar ratio of 1.67. Its composition is close to the inorganic constituent of mineralized bone tissue. Many studies demonstrated the biocompatibility of hydroxyapatite [1, 2]. However, in spite of the numerous investigations the mineral host response is not fully understood. Some authors emphasize the importance of the crystal size of the bioceramic [3]. Others postulate that dissolution/reprecipitation and/or epitaxial growth might be the dominating factor [8–10]. Several reports indicated a direct contact between the implanted synthetic calcium phosphate and bone tissue [2, 8], whereas authors related also an electron-dense layer interposed between the ceramic and bone tissue [3, 11].

However, one of the main problems linked to the use of ceramics lies in the difficulty of machining dense hydroxyapatite [12]. Thus, it is often used in the form of granules with the drawback of easy migration away from the surgical area. Many procedures have been evaluated for avoiding the loss of bioceramic powders and/or increasing their properties [13, 14].

TenHuisen and Brown [15, 16] developed recently hydroxyapatite gelatin composites consisting of a gelatin network interconnecting hydroxyapatite clusters [15] and hydroxyapatite-ionomer cements [16]. Since setting and hardening of both products can occur at physiological temperature and in the presence of biological fluids, their use in the dental fields can be envisaged.

Iyoda *et al.* [17] assessed the effectiveness of cultured chondrocytes bound to porous synthetic hydroxyapatite as a bone implant material, whereas Marggraf *et al.* [6] implanted a hydroxyapatite–collagen composite in bone defects. This paper deals with the long-term behaviour of a commercially available hydroxyapatite/collagen–glycosaminoglycan biomaterial (Biostite®), which is more or less comparable to mineralized bone tissue. Biostite® has been placed in a freshly extracted tooth alveoli in man, to promote the gain of bone and make later endosseous implantation feasible. The aim of our study was to

0957–4530

evaluate the transformations undergone by the post-implanted material, and to compare host responses with the findings in the literature for implants of hydroxyapatite alone.

2. Materials and methods

2.1. Implant material

A hydroxyapatite/collagen–glycosaminoglycan composite (Biostite®, Pred, Levallois-Perret, France) was used for the filling of a freshly extracted alveoli. The mineral component (synthetic hydroxyapatite) of the implant material was prepared according to the double decomposition technique developed by Trombe (1972) [2, 18], with particle sizes ranging from ten to several hundred micrometres. Each hydroxyapatite particle is formed by numerous individual crystallites with variable size ranging from about ten to several hundred nanometres.

The synthetic hydroxyapatite powder was blended or coated with 9.5% collagen, extracted from calf skin and 2.5% chondroitin 4-sulphate, a glycosaminoglycan of ovine origin (Translagène®, Bioetica, Lyon, France). The collagen consisted of 97% of type I collagen and 3% of type III collagen [18].

2.2. Clinical procedures

Biostite® was placed in the alveolar socket immediately after extraction of the upper left first premolar of a 40-year-old female. The flap was then firmly sutured in place. Postsurgical care by the patient consisted of twice daily chlorhexidine (0.1%) mouth-rinsing for 2 weeks. Healing of the surgery site was satisfactory. A biopsy specimen of the filled alveolar socket was retrieved after 42 months and just before the endosseous implantation surgery, for prosthodontical purposes.

2.3. Tissue preparation and methods of study

The biopsied specimen was immediately fixed in a 2% paraformaldehyde–glutaraldehyde solution buffered at pH 7.4 with 0.1 M sodium cacodylate, and post-fixed in a 1% osmium tetroxide solution in the same buffer. The specimen was then divided in two parts. One half of the fixed specimen was prepared for transmission electron microscopy (TEM), while the other fraction was submitted to scanning electron microscopic (SEM) preparation techniques.

For TEM, the specimen was embedded in Epon 812. Ultrathin sections without decalcification were prepared with a microtome (Sorvall® MT1, Porter-Blum) equipped with a diamond knife. If staining was needed, it was performed with uranyle acetate and lead citrate. High resolution electron microscopy observations were obtained with sections deposited on carbon-coated holey formvar-covered 1000 mesh grids. Conventional TEM was realized with a JEOL 100B equipped with a cooled trap at either 60 kV or 100 kV, while high resolution TEM examination was realized with a Philips EM 430 ST working with a LaB_6 cathode at 300 kV. This microscope has a Scherzer resolution of 0.19 nm. The high-resolution TEM micrographs were systematically analysed with an optical bench (Micro-Contrôle, France) using a helium–neon laser, which allows checking for astigmatism and the determination of lattice plane equidistances as well as the zone axes of the observed crystals.

Three different techniques were used for sample preparation of the SEM study. The crude biomaterial was simply cut with a lancet, metal coated and then observed with the SEM. Flat surfaces were prepared from Epon embedded biopsy blocks after cutting with a diamond knife as for TEM. The surface was then metal-coated and observed as before. Other biopsy specimens were fixed as mentioned previously, dehydrated in an ethanol series (from 70% to 100%) and cryofractured after freezing in liquid nitrogen. All SEM samples were coated with a gold–palladium alloy by cathodic sputtering (Hummer-Junior, Siemens, Germany) and observed in a JEOL 35C at 25 kV.

The crude Biostite® biomaterial was also analysed by X-ray diffraction (Siemens D500) using the CuK_α radiation ($\lambda_{CuK_\alpha} = 0.154$ nm), and compared with JCPDS powder diffraction files (9-432 of hydroxyapatite).

3. Results

During the 42 months of implantation of the biomaterial wound healing was uneventful and no clinical complaint was noted from the patient. Scanning electron microscopy (SEM) and transmission electron microscopy (TEM) studies were made of both the implanted and non-implanted material.

Fig. 1 shows the non-implanted composite (Biostite®) which is constituted of mineral particles with irregular outlines and rough surfaces. This mineral component appears to be integrated in an organic matrix formed mainly by interwoven fibres. After embedding and sectioning the crude implant material, transmission electron microscopy (TEM) showed that each mineral particle was made up of numerous single crystals and electron-lucent intercrystalline spaces (Fig. 2). The size of these synthetic crystals was highly variable, ranging from ten to several hundred nanometres.

When the raw composite material was analysed using X-ray diffraction, a perfect concordance with the hydroxyapatite theoretical parameters was evident (Fig. 3a). Using magnified TEM images, lattice values of the individual synthetic hydroxyapatite crystals could be estimated (Fig. 3b), after defining the observation axis by optical diffraction pattern (Fig. 3c). The (1 0 0) planes with 0.82 nm interreticular distances could be clearly seen.

SEM investigations of the freeze-fractured biopsy, after 42 months implantation in a human freshly extracted alveolar socket, showed hydroxyapatite particles comparable to those observed prior to implantation (Fig. 4a). These hydroxyapatite aggregates retained a granular appearance with a fibrous tissular interface. When the same biopsy was embedded and sectioned with a diamond knife, SEM revealed

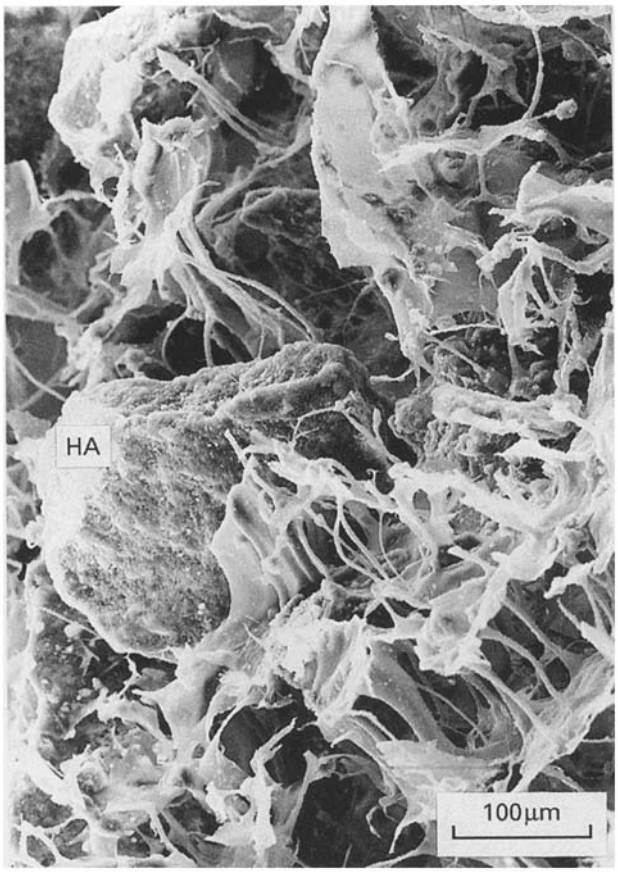

Figure 1 Scanning electron microscopic (SEM) view showing the three-dimensional organization of the composite material before implantation. Hydroxyapatite particles (HA) with irregular shapes and granular surfaces are surrounded by a fibre network.

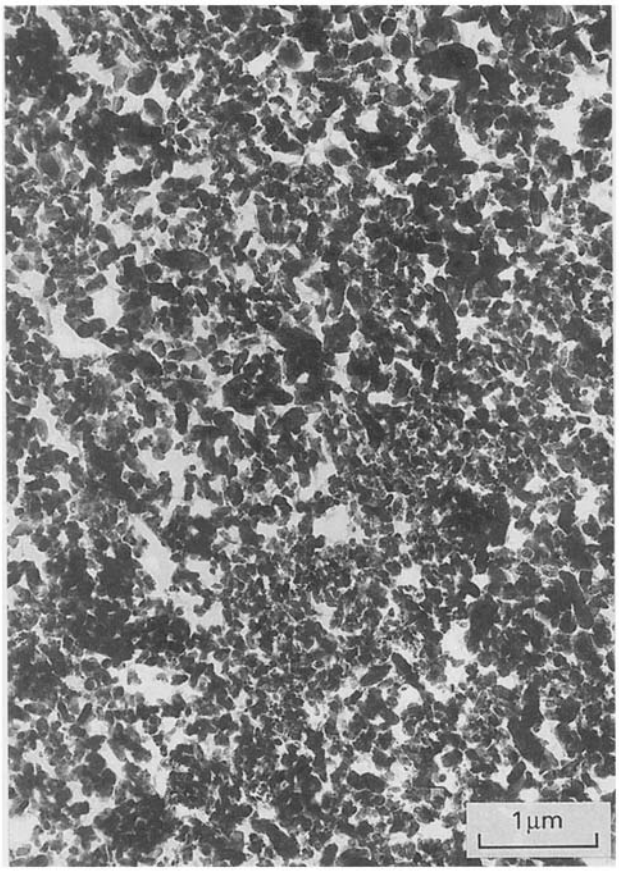

Figure 2 In transmission electron microscopy (TEM) each of the hydroxyapatite particles seen in Fig. 1 appears as an aggregate of numerous individual crystals.

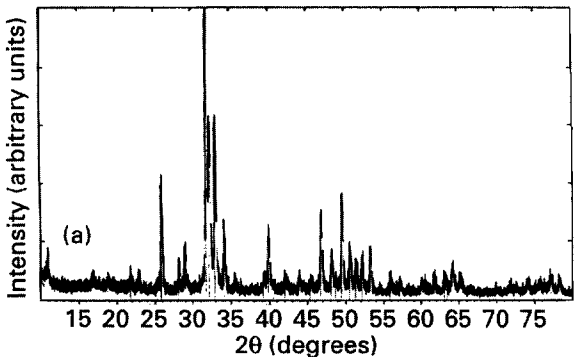

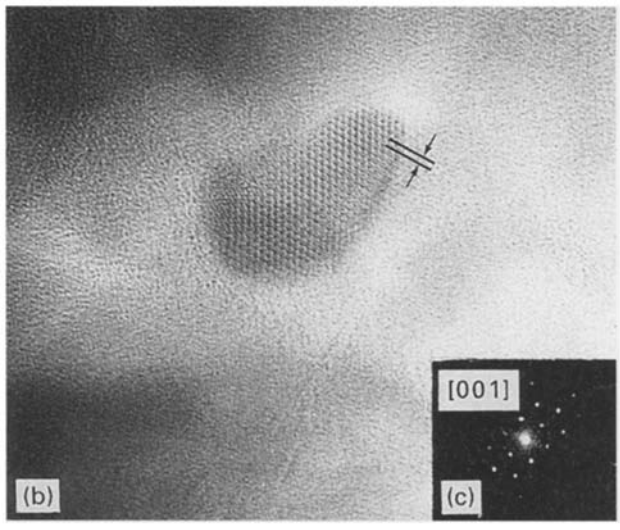

Figure 3 (a) X-ray diffraction diagram of the composite implant material with a perfect correspondence to the hydroxyapatite data. (b) High resolution TEM micrograph of a hydroxyapatite crystal prior to implantation revealing periodic lattice fringes of 0.82 nm related to the (1 0 0) planes. (c) Optical diffractogram of the crystal from Fig. 3b corresponding to the [0 0 1] zone axis.

irregularly shaped particles of many different sizes, surrounded by soft tissue (Fig. 4b). The implanted hydroxyapatite aggregates also exhibited different grey levels, which could be the consequence of localized mineral responses. Two different response types could be observed. In the first, the calcification of the intercrystalline spaces was clear (Fig. 5). A large number of freshly formed small crystals of size similar to the adjacent alveolar bone crystals occupied the spaces left between the synthetic hydroxyapatite crystals. The hollow areas were artifacts due to the preparation process. In some cases, the implanted particles with completely calcified intercrystalline spaces were in close contact with a peripheral mineralized layer (Fig. 6) The intercrystalline mineral deposits merged with the outer calcification area. The evaluation of the osseous condition, only a few months after tooth extraction and filling the alveolar socket with Biostite®, is shown in Fig. 7a. The 42-months post-implantation biopsy showed an irregular mineralization response at the periphery of the implanted aggregates. In some cases, calcified deposits at the hydroxyapatite particle boundaries formed a very thin layer of several hundred nanometres (Fig. 7b). The layer itself was composed both of more mature crystallites and of very tiny mineralized ribbons comparable to those found in developing bone areas. On the other hand, the outer

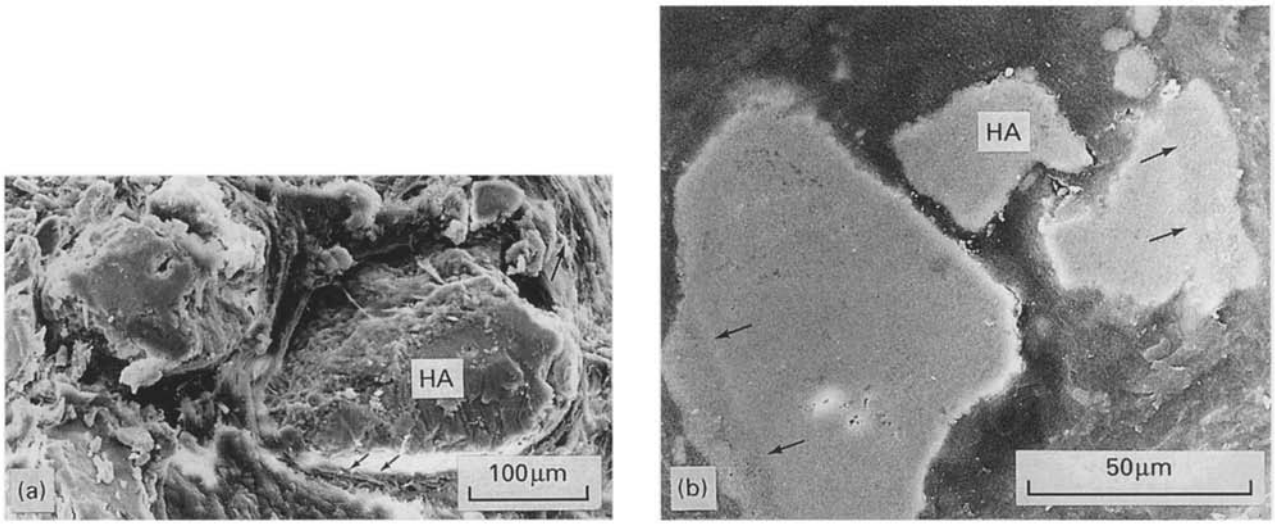

Figure 4 (a) SEM observation of a cryofractured biopsy of the implant material 42 months after implantation. The hydroxyapatite particles (HA) look similar to those of the initial biomaterial, and are surrounded by a fibre-rich tissue (arrows). (b) Scanning electron microscopy of an Epon-embedded biopsy, sectioned with a diamond knife. The irregular shaped hydroxyapatite aggregates seem incorporated in a soft tissue. The arrows indicate possible localized mineral responses. 42 months after implantation.

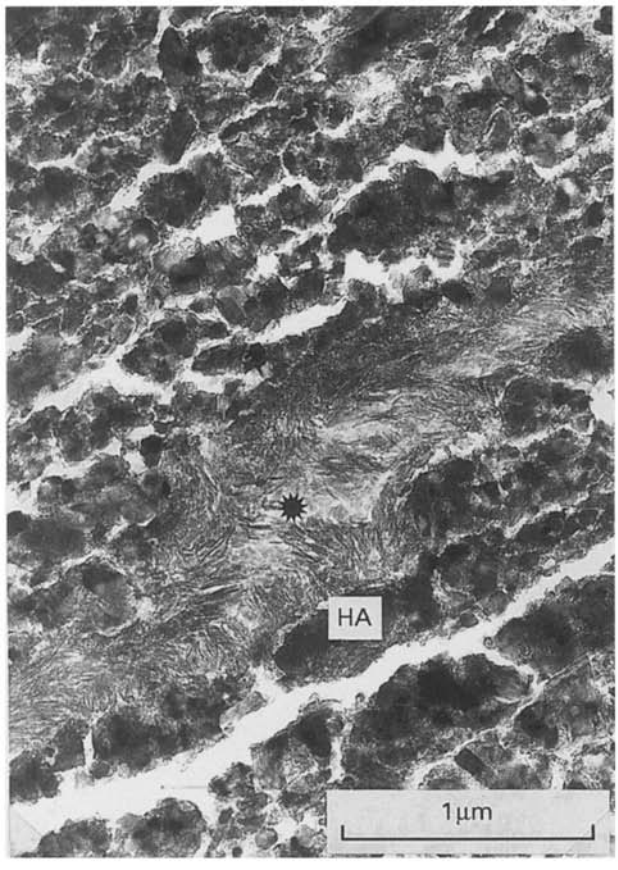

Figure 5 TEM observation of a hydroxyapatite particle recovered after 42 months. The intercrystalline spaces between the implanted synthetic crystals (HA) are filled with newly formed minute crystals (star).

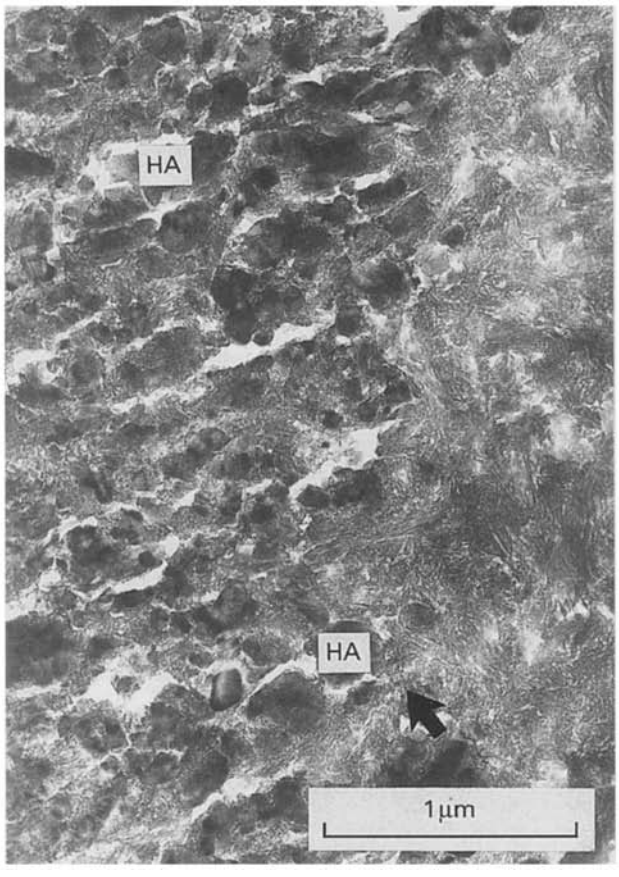

Figure 6 TEM of the peripheral area of an implanted hydroxyapatite particle. The mineral deposits between the synthetic crystals (HA) are in continuity (arrow) with calcified tissue.

mineralization was in direct continuity with lamellar bone (Fig. 8). The large collagen fibrils of this mineralized matrix were oriented roughly parallel, and the typical 64 nm cross-bandings could be seen. In the second response type, absolutely no mineralization had taken place in the spaces between the implanted hydroxyapatite crystals (Fig. 9). The post-implanted aggregates were made up of numerous crystallites with widely varying dimensions, similar to the crude biomaterial. In addition, those implanted hydroxyapatite particles were incorporated in soft tissue and the electron-lucent intercrystalline spaces seemed filled with an organic stroma of amorphous appearance. Other implanted aggregates were separated from the calcified bone matrix by an unidentified soft tissue (Fig. 10). As with SEM (Fig. 4b), a partial, localized

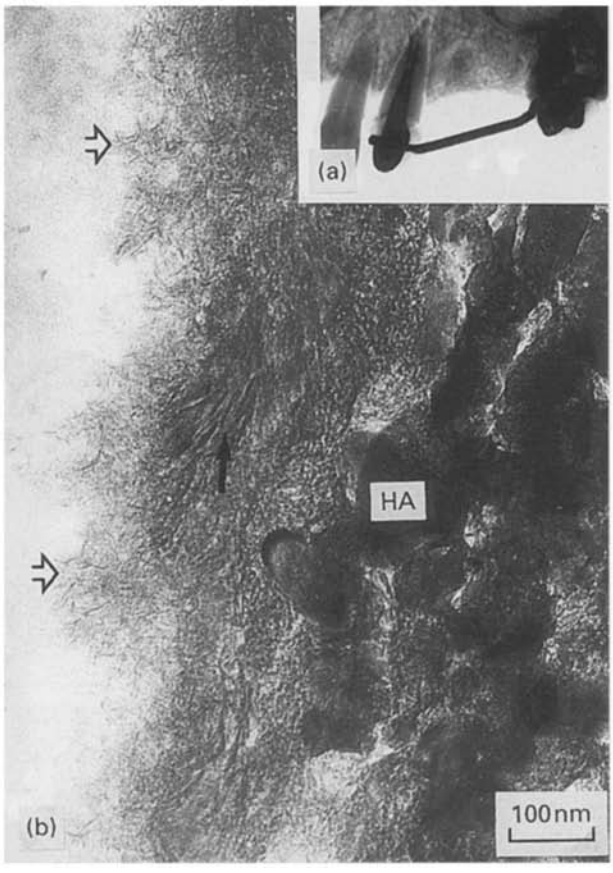

Figure 7 (a) Radiograph realized 5 months after implantation of the hydroxyapatite–collagen composite material in the freshly extracted alveoli. (b) TEM observation of freshly formed crystals at the surface of an implanted aggregate of synthetic hydroxyapatite crystals (HA) removed after 42 months. This calcified layer exhibits either very early mineralization stages (hollow arrows) or more mature crystals (arrow).

Figure 8 Non-decalcified ultra-thin section showing the peripheral bone layer with well-oriented collagen fibrils. Note the presence of periodic striations reminiscent of the latter (arrows).

calcification process could also be observed using TEM (Fig. 11). One border of the synthetic hydroxyapatite particle was in close contact with calcified bone tissue having an ordered collagenous matrix, while the opposite side of the aggregate was surrounded by soft tissue. In this case, the spaces between the synthetic crystals were only partly mineralized. In other areas, dense spherical calcified foci could be observed within the osteoid tissue at the periphery of an implanted hydroxyapatite aggregate, with intercrystalline spaces remaining mostly unmineralized (Fig. 12). The needle-like crystals of the calcified islands seemed oriented along the collagenous fibrils. In addition, it must be mentioned that neither intracellular nor extracellular dissolution of the implanted hydroxyapatite crystals could clearly be observed.

4. Discussion

The main purpose of filling extraction sites with hydroxyapatite-containing biomaterials is to promote bone formation, and thus to allow further endosseous implantation as the support of a prosthodontical construction. Ultrastructural assessments of the biomaterials before and after implantation seem to be of prime importance in determining their possible benefits. To our knowledge, only a few studies have been carried out on such materials, using essentially optical microscopy. Our results are quite comparable to data

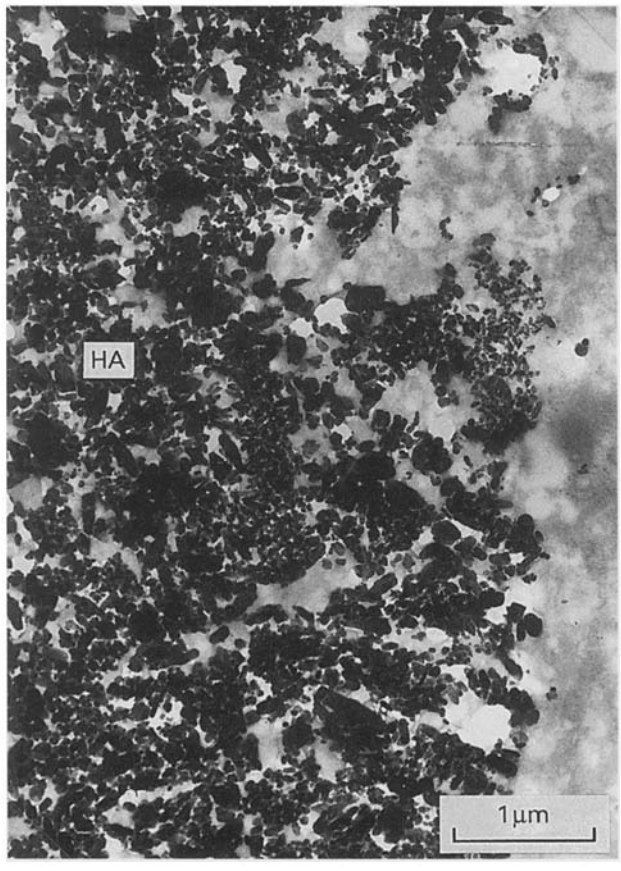

Figure 9 TEM micrograph showing a hydroxyapatite particle after 42 months of implantation. The implant material is in close contact with soft tissue. Note the absence of mineralization between the individual crystals (HA).

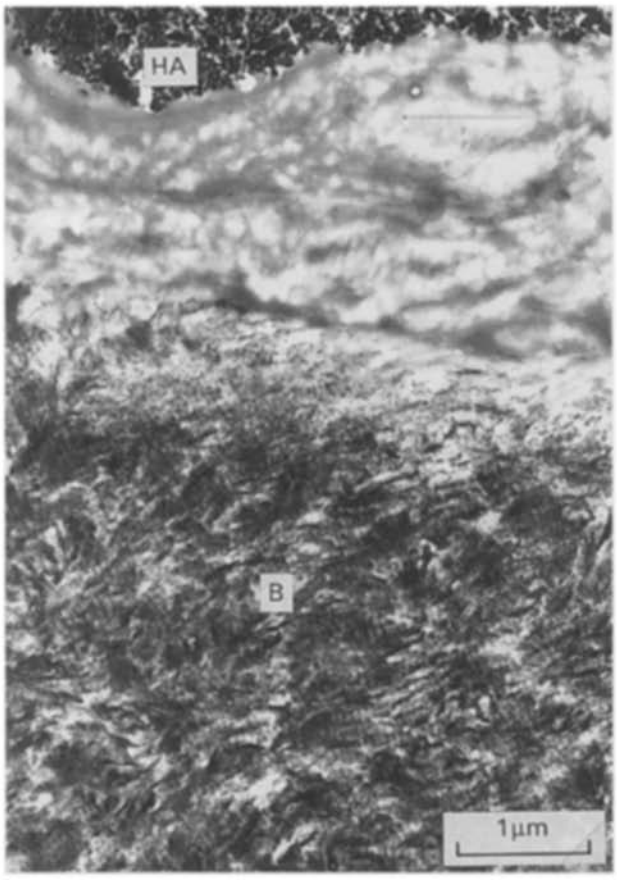

Figure 10 Soft tissue separating an implanted aggregate of hydroxyapatite crystals (HA) from calcified bone (B).

Figure 11 TEM observation of bone apposition with well-oriented collagen fibrils (B) along a hydroxyapatite particle implanted for 42 months. Only some intercrystalline spaces (circle) are filled with mineral material. The opposite border of the implanted aggregate (arrows) interfaces with soft tissue.

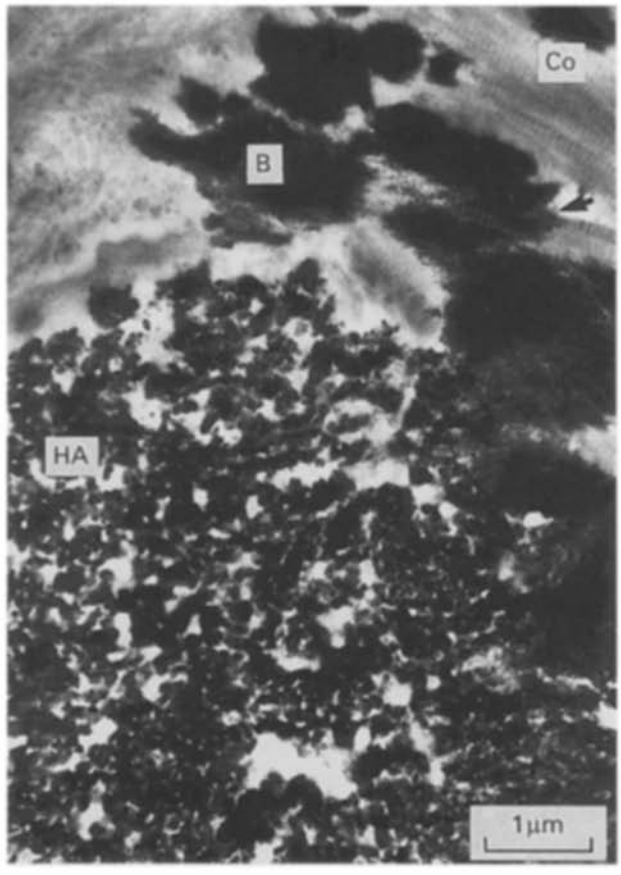

Figure 12 TEM micrograph showing (after 42 months implantation in a human alveolar socket) a hydroxyapatite particle (HA) surrounded by an osteoïd tissue (Co) with several spherical bone islands (B). Note the mineralizing collagen fibrils (arrow). Most of the spaces between the implanted crystals remain uncalcified.

previously described [18] (Figs 4 and 11). After 3 months of Biostite® implantation in experimental periodontal lesions, using the beagle dog model, Frank *et al.* [18] demonstrated that the synthetic hydroxyapatite particles were not integrated in the alveolar bone, but were rather encapsulated in a fibrous connective tissue. Glycosaminoglycans play significant roles in the mineralization of biological hard tissues. They possess negatively charged sulphate and/or carboxylate groups. The relationship of glycosaminoglycans such as chondroitin sulphate and the dissolution properties of hydroxyapatite have already been reported [19]. These authors suggested an ion exchange mechanism between the phosphate ions at the hydroxyapatite surface and the anionic groups of glycosaminoglycans adsorbed on the mineral, as well as the binding of calcium ions to free glycosaminoglycan in the solution. Collagen has also been used before in relation with hydroxyapatite and bone defects [6]. When this protein was used as a carrier of bone morphogenetic protein and then implanted, it was shown to be gradually degraded and replaced by new bone [20]. According to electron microscopic investigations, the implanted collagen provided space for newly formed collagen and the invading cells. Calcium phosphate ceramics are considered as very compatible materials from the standpoint of hard tissue response [21]. The calcium phosphate component of the Biostite® prior to implantation, namely hydroxyapatite (Fig. 3a), appeared

dispersed in a fibrous organic matrix (Fig. 1). This structure could lead to the ingrowth of tissue and the supplying of blood vessels. On the other hand, the spaces smaller than 1 μm found between the well crystallized hydroxyapatite crystals (Figs 2 and 3) are supposed to allow the formation of bone-like needle-shaped crystals [2, 8]. The latter mineralization process was also observed in some of the hydroxyapatite aggregates within the analysed biopsy (Figs 5 and 6). A survey of the literature reveals several descriptions of this calcification phenomenon. In particular, a dissolution/reprecipitation mechanism was advanced. Daculsi *et al.* [8] mentioned the formation of bone-like apatite crystals, apparently due to the precipitation of the calcium and phosphate ions released by the dissolution of the ceramic crystals. Bagambisa *et al.* [10] described the formation of a recrystallisation layer of spherocrystallites. Ogiso *et al.* [9] related an initial calcification by inorganic epitaxy at the surface of dense hydroxyapatite. However, in the present study the newly formed crystals growing between the synthetic hydroxyapatite crystals were not systematically found in all implanted aggregates (Fig. 9). Furthermore, around some aggregates bone apposition occurred within peripheral osteoid tissue prior to the mineralization of the intercrystalline spaces in the hydroxyapatite particles (Fig. 12). Others [2] came to the same conclusion when hydroxyapatite alone was used as implant material. The host response at the periphery of the synthetic crystal aggregates seemed quite irregular (Figs 4 and 11). It was possible to observe well-mineralized areas (Figs 6 and 8), while other hydroxyapatite particles remained in contact with soft tissue (Fig. 9), or were separated from a calcified matrix by a non-mineralized layer (Fig. 10). Even though many reports demonstrated cell-mediated resorption of the calcium phosphates both *in vitro* [22–24] and *in vivo* [2, 25], such degradations were not evident for Biostite® after long implantation periods. In several studies a significant dissolution rate of the ceramic crystals was emphasized [24, 26]. Surfaces and crystal core dissolutions were demonstrated and it was suggested that the crystal defects were the starting points of the degradation mechanism [26]. Such phenomena were not found for the hydroxyapatite crystals of the implanted Biostite® (Figs 2 and 9). In the present study attention was mainly directed to the calcification process. In spite of the apparently satisfactory postoperative radiographs, the ultrastructural investigations suggest that an organic matrix interspersed with hydroxyapatite crystal aggregates was not more efficient (than other calcium phosphate biomaterials) for gaining new bone.

5. Conclusions

The ultrastructural analysis of a biomaterial (Biostite®) recovered 42 months after implantation in a human freshly extracted tooth alveoli provided us with significant information about the host responses and the long-term behaviour of a hydroxyapatite/collagen–glycosaminoglycan biomaterial. Mineral response was irregular and only localized. Further, the synthetic hydroxyapatite involved in this composite material appeared to be not readily resorbable.

Acknowledgement

The authors thank H. Zins for typing the manuscript.

References

1. E. P. BENQUE, M. GINESTE and M. HEUGHEBAERT, *J. Biol. Buccale* **13** (1985) 271.
2. A. OGILVIE, R. M. FRANK, E. P. BENQUE, M. GINESTE, M. HEUGHEBAERT and J. HEMMERLE, *J. Periodont. Res.* **22** (1987) 270.
3. R. M. FRANK, P. KLEWANSKY, J. HEMMERLE and H. TENENBAUM, *J. Clin. Periodont.* **18** (1991) 669.
4. G. DACULSI, N. PASSUTI, S. MARTIN, J. C. LE NIHOUANNEN, V. BRULLIARD, J. DELECRIN and B. KEREBEL, *Revue de Chirurgie Orthopédique* **75** (1989) 65.
5. J. M. TRIGLIA, C. SCHEINER, J. GOUVERNET and M. CANNONI, *Arch. Otolaryngol Head Neck Surg.* **119** (1993) 87.
6. E. MARGGRAF, H. NEWESELY and R. HOSEMANN, *Dtsch Zahnärztl Z.* **40** (1985) 28.
7. R. M. FRANK, P. WIEDEMANN, J. HEMMERLE and M. FREYMANN, *J. Appl. Biomater.* **2** (1991) 243.
8. G. DACULSI, R. Z. LEGEROS, E. NERY, K. LYNCH and B. KEREBEL, *J. Biomed. Mater. Res.* **23** (1989) 883.
9. M. OGISO, T. TABATA, T. ICHIJO and D. BORGESE, *J. Long-Term Effects Medical Implants* **2** (1992) 137.
10. F. B. BAGAMBISA, U. JOOS and W. SCHILLI, *J. Biomed. Mater. Res.* **27** (1993) 1047.
11. J. D. DE BRUIJN, C. P. A. T. KLEIN, K. DE GROOT and C. A. VAN BLITTERSWIJK, *ibid.* **26** (1992) 1365
12. M. Y. SHAREEF, P. F. MESSER and R. VAN NOORT, *Biomaterials* **14** (1993) 69.
13. C. A. VAN BLITTERSWIJK, J. R. DE WIJN, H. LEENDERS, J. V. D. BRINK, S. C. HESSELING and D. BAKKER, *Cells and Materials* **3** (1993) 11.
14. M. SAITO, A. MARUOKA, T. MORI, N. SUGANO and K. HINO, *Biomaterials* **15** (1994) 156.
15. K. S. TENHUISEN and P. W. BROWN, *J. Biomed. Mater. Res.* **28** (1994) 27.
16. *Idem., J. Dent. Res.* **73** (1994) 598.
17. K. IYODA, T. MIURA and H. NOGAMI, *Clin. Orthop. Rel. Res.* **288** (1993) 287.
18. R. M. FRANK, J. F. DUFFORT, E. P. BENQUE and J. L. LACOUT, *J. Parodontologie* **10** (1991) 255.
19. H. TANAKA, T. ARAI, K. MIYAJIMA, S. SHIMABAYASHI and M. NAKAGAKI, *Colloids and Surfaces* **37** (1989) 357.
20. Y. HORISAKA, Y. OKAMOTO, N. MATSUMOTO, Y. YOSHIMURA, A. HIRANO, M. NISHIDA, J. KAWADA, K. YAMASHITA and T. TAKAGI, *J. Biomed. Mater. Res.* **28** (1994) 97.
21. G. HEIMKE and P. GRISS, in "Bioceramics of calcium phosphate". edited by K. de Groot (CRC Press, Boca Raton, FL, 1983) pp. 79–97.
22. K. GOMI, B. LOWENBERG, G. SHAPIRO and J. E. DAVIES, *Biomaterials* **14** (1993) 91.
23. J. E. DAVIES, D. SHAPIRO and B. F. LOWENBERG, *Cells and Materials* **3** (1993) 245.
24. J. D. DE BRUIJN, Y. P. BOVELL, J. E. DAVIES and C. A. VAN BLITTERSWIJK, *J. Biomed. Mater. Res.* **28** (1994) 105.
25. M. F. BASLE, D. CHAPPARD, F. GRIZON, R. FILMON, J. DELECRIN, G. DALCULSI and A. REBEL, *Calcif. Tissue Int.* **53** (1993) 348.
26. G. DACULSI, R. Z. LEGEROS and D. MITRE, *Calcif. Tissue Int.* **45** (1989) 95.

Received 15 August
and accepted 19 October 1994